Electronic structure, ferromagnetism, and EELS spectra of crystalline alloys Fe_nB and Ni_nB (n=1,2,3): Aspects of universal behavior

A. M. Bratkovsky
Research Centre in Superconductivity, University of Cambridge, Madingley Road, Cambridge CB3 OHE, United Kingdom

S. N. Rashkeev* and G. Wendin
Institute of Theoretical Physics, Chalmers University of Technology, S-412 96 Göteborg, Sweden
(Received 13 January 1993; revised manuscript received 26 April 1993)

We have performed an extensive study of the electronic structure, optical properties, and electron-energy-loss spectra (EELS) for the series of the M_3B, M_2B and MB, (M=Fe, Ni) crystalline alloys. The electron density of states (DOS) of iron and nickel borides of the same composition have almost the same shape in spite of some minor differences in actual atomic structures. The Fermi level in nickel borides is shifted upwards in comparison with its position in iron borides, away from the main DOS peak formed by the nonbonding M d states. This behavior provides insight into the "marginal" stability of the nickel magnetic moment upon dilution by nonmagnetic atoms. As a result of competitive interaction between d-d metallic bonding and d-p M-metalloid covalent bonding the magnetic moment on the Fe atom gradually decreases with increasing boron content. This tendency is in accordance with the results of a simple generalized Stoner theory, which is capable of describing the ferromagnetic behavior in detail with good accuracy for the estimated magnetic moments. In spite of some differences in actual crystal structure and a high degree of crystalline anisotropy, the calculated EELS spectra are practically identical for all iron compounds studied. The spectra are dominated by a giant peak at about 20 eV, with some fine structure at lower energies (at about 10 eV) relevant to B p–M d transitions. The d-d transitions appear to be very strong in the low-energy region (0–10 eV) leaving the usual Drude term effective only at energies below 1.5 eV. These transitions suppress the low-energy plasmons both in para and ferromagnetic phases and make just small differences in the calculated EELS spectra, in accordance with the available experimental data. The implications of the present results for the amorphous systems are discussed.

I. INTRODUCTION

Almost six decades of experimental studies of transition metal (M) borides still leave many questions to be resolved with regard to structural, physical, and chemical properties. The presence of boron chains in some of the borides allowed Kiessling[1] to postulate a covalent interaction between the boron atoms. This is likely to be responsible for the complicated unit cells[2] and interesting physical properties of borides, many of which remain a matter of debate. The borides are characterized by technologically important properties such as great hardness, high melting points, glass-forming ability,[3] an Invar behavior,[4,5] and a strong magnetovolume effect,[6] besides the fact that borides are members of a novel family of permanent magnets ($R_2Fe_{14}B$, where R = rare-earth element).[7]

The magnetic properties of the M-B compounds are very interesting and still represent a challenge for theory, especially amorphous systems exhibiting soft magnetic behavior important for applications. Crystalline Fe-B and Co-B alloys are itinerant ferromagnets where the magnetic moment on a transition-metal atom gradually decreases from its maximum value in pure Fe and Co down to zero value with increasing B content.[8,9] Thus, the moment on Fe in 50:50 compounds is about 50% of its value in bcc Fe, whereas CoB is paramagnetic. The moment on Ni is "marginal," and crystalline Ni_3B already behaves as a Pauli paramagnet.[10–12]

Perhaps, remarkably, the magnetic properties of transition-metal–metalloid crystalline compounds are very similar to those of amorphous counterparts with the same composition (see Refs. 9–14 for a review of magnetic glasses). This might signal a close similarity between the electronic structures of both phases, as seen by high-resolution uv photoemission, Auger electron and energy-loss spectroscopy (see Refs. 15, 10 and 11 and references therein).

There exists a long-lasting controversy about the magnetic behavior of the iron-rich Fe-B glasses. Namely, some studies of amorphous $Fe_{100-x}B_x$ alloys suggest a more or less monotonous increase of the moment on the Fe atom μ_{Fe} with decreasing x to a value close to that of crystalline α-Fe, while the others suggest that there is a maximum value of μ_{Fe} at $x \approx 20$ and then the moment decreases down to $\approx 1.5\mu_B$/Fe in the hypothetical

pure amorphous Fe (both groups of the data were thoroughly analyzed in Ref. 16). The latter value might be compared with the semiempirical tight-binding Hubbard model calculations of Krey and co-workers which give reduced ferromagnetism for amorphous Fe ($\mu_{Fe} \approx 1.2\mu_B$) (Ref. 17) and a featureless density-of-state (DOS) shape for $Fe_{80}B_{20}$.[18] Recently, Kakehashi has claimed a genuine spin-glass behavior with vanishing net magnetic moment for iron-rich amorphous systems on the basis of semiempirical finite-temperature Hubbard-model calculations.[19] These calculations are, however, in disagreement with first-principles local-spin-density (LSD) supercell estimates, which give $\approx(2.3\text{–}2.46)\mu_B$/Fe for the net moment in amorphous Fe.[20,21] It should be mentioned that the DOS shape calculated within the Hubbard model[18] cannot account for all the peaks clearly seen in the high-resolution photoemission data.[15] The amorphous magnetism in Fe-B systems has been extensively studied by Bratkovsky and Smirnov with the real-space spin-polarized tight-binding linear muffin-tin-orbital (LMTO) method.[22,23] The method is a version of the standard LMTO method[24] where the extended basis set is transformed into a *most localized* form,[25] and used in combination with the recursion method.[26] The results show an itinerant magnetism in the glasses Fe-B with magnetic moments on iron sites reaching its maximum value in the (hypothetical) amorphous iron ($2.25\mu_B$). The net iron moment gradually decreases upon dilution by boron, approaching a zero value at the critical composition $Fe_{40}B_{60}$.[23] The calculated value of the moment in $Fe_{80}B_{20}$, 2.1 μ_B/Fe,[22] is in good agreement with experiment and the value estimated from the generalized Stoner criterion applied to the paramagnetic DOS of $Fe_{80}B_{20}$, $2.2\mu_B$/Fe.[27] The discrepancy between the LSD and Hubbard-model calculations has provided additional motivation for carrying out extensive first-principles calculations of the electronic structure and properties of crystalline borides.

So far, very few previous first-principles spin-polarized studies of the electronic structure of borides have been performed. Mohn and Pettifor[28] have presented augmented-spherical-wave (ASW) results for the series of MB and M_2B alloys with transition metals M from $3d$ and $4d$ series. The electronic density of states of FeB, Fe_2B, and Fe_3B has also been calculated with the use of the orthogonalized linear-combination-of-atomic-orbitals (OLCAO) method.[29] Paramagnetic DOS calculations have been done for FeB and Fe_2B by the linearized augmented-plane-wave (LAPW) method[30] and for Fe_2B by the LMTO method.[27]

Concentrating on the magnetic properties of borides, we should recall the earlier picture of borides where the behavior of the magnetic moment was explained as a result of electron transfer from the metalloid atom gradually filling in the M d band.[31] Similar arguments were evoked to explain the observed trends in magnetic glasses M-M' (M'=B, P, and C).[32–34] X-ray experiments on FeB and Fe_2B crystals have provided evidence that this simplified picture does not hold, the electronic configuration significantly deviates from spherical symmetry, and the bonding of unlike atoms has a covalent nature and *not* ionic.[35] The corresponding covalent M d-B p interaction was used to explain the observed moment distribution over the unit cell.[35] As for the charge transfer, previous LSD calculations are in disagreement: Nowak *et al.*[27] have argued that B donates 0.42 electron to Fe in Fe_2B and 1.0 electron in amorphous $Fe_{80}B_{20}$, but in Ref. 29 0.5–0.6 electrons are transfered *from* Fe *to* B. Here we are able to demonstrate the effects of p-d hybridization and establish that some moderate charge transfer takes place *from* B *to* Fe (Sec. II A).

The stability and magnetic properties of these systems are ruled by both B p–B p and M d–B p interactions as described by Gelatt, Williams, and Moruzzi[36] and Weaver, Franciosi, and Moruzzi.[37]. It is well known that with increasing B content there evolve boron zigzag chains infinitely expanding through FeB and NiB crystals.[1,2] As the transition-metal host is diluted by boron the d–d bonding becomes weaker, but simultaneously d states interact with metalloid s and p states, forming bonding and antibonding hybrids which can be more effective in bonding than the parent states. The bonding mechanism strongly affects the formation of ferromagnetic states. Any gain in exchange energy due to ferromagnetic splitting in d bands is accompanied by a loss in d-p bond energy.[28] The pronounced covalent character of the bonding might imply an inhomogeneous electron-density distribution, and there might be feedback effects on the electron DOS and polarization. To gain more insight into that matter, we have undertaken full-potential LMTO calculations[38] to take complete account of the nonspherical part of the electron density, and it turned out that the precision of the present atomic sphere approximation (ASA) calculations is very high. The bulk of our results will be presented, therefore, for the ASA-LMTO calculations where an electronic potential is constructed from a spherically symmetric part of the density.[24]

We shall next address the origin of itinerant ferromagnetism in iron borides and the paramagnetic behavior of nickel borides (Sec. II B). We shall show that the Fermi energy in the iron systems studied here is always pinned above pure d states. Therefore, the generalized Stoner model[27] is applicable and reproduces the M moments with good accuracy, including the absence of moments on Ni atoms in all compounds studied. The overall behavior of Fe- and Ni-based borides turns out to be very similar and almost follows a rigid-band picture apart from some minor details.

Finally, we shall discuss the optical properties of these compounds with emphasis on electron-energy-loss spectra (EELS), which, to the best of our knowledge, have not been reported previously (Sec. III). One would have expected that the dipole (optical) transitions into the M p states lying well above the Fermi level from the M d states near E_F will dominate. However, we will show later that these transitions have only a minor effect on the EELS. This fact explains a peculiar behavior of EELS, which contains a plasmon peak dominating at energies $\approx$20 eV. This energy scale is generic for *all* studied compounds, which explains the experimental evidence that the effect of ferromagnetic splitting is practically not seen.[15]

II. TRENDS IN THE PARAMAGNETIC ELECTRON DENSITY OF STATES AND THE GENERALIZED STONER MODEL

A. Paramagnetic DOS

Let us start with the discussion of MB compounds. They crystallize either in the FeB or in the CrB structure (NiB) with 4 f.u. in an orthorhombic unit cell. The FeB space group is *Pbnm* with all atoms in symmetry planes. An interesting feature of the FeB structure is the direct contact of each boron atom with two neighbors 1.77 Å apart, which can be seen as a zigzag chain extending through the crystal. The iron atom is well coordinated by six iron atoms at a distance of 2.72 Å and four further iron atoms at 2.85 Å. The NiB structure (CrB type) can be seen as a distorted variant of the FeB structure with the space group *Cmcm*.

Fe_2B and Ni_2B have the Al_2Cu structure (*I*4/*mcm*) with 2 f.u. in a body-centered tetragonal unit cell. The structure can be viewed as consisting of alternating Fe and B planes. There are no boron chains as boron atoms are farther apart in comparison with the FeB structure and have a nearest neighbor at 2.12 Å. Ni_3B is of the cementite type Fe_3C (Ref. 2) with 4 f.u. per orthorhombic cell. Fe_3B crystallizes in the cementite and in the body-centered tetragonal (bct) phase.[13] Although the bct phase is believed to be somewhat more stable, we have considered the cementite structure for the Fe_3B compound.[2] There are two inequivalent positions for the Fe atoms, no direct B-B contact, and the Fe-Fe distances vary between 2.51 and 2.76 Å.

We have included s, p, and d orbitals for Fe(Ni) and B in the calculation of the self-consistent electronic density. For the calculation of the observable spectral characteristics such as EELS we have also added the f orbitals for Fe(Ni) because the d-f transitions on the M site have very large oscillator strength and play an important role in the formation of the frequency-dependent dielectric function. We have also included the M f orbitals into a self-consistent scheme when calculating the electronic density and the magnetic moments in the ferromagnetic phases by the local-spin-density-functional approximation (LSDA) ASA-LMTO procedure to improve the accu-

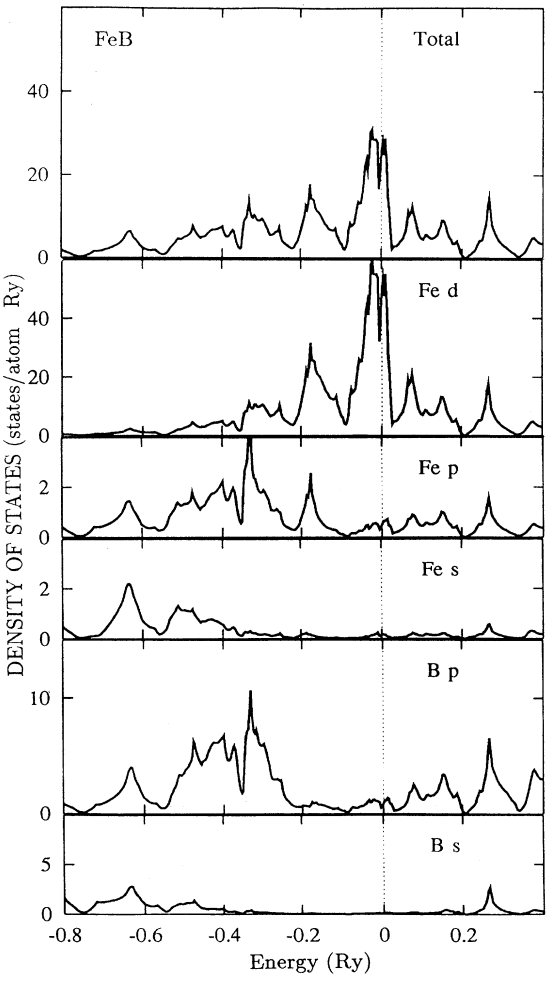

FIG. 1. Paramagnetic density of states of FeB (s_{Fe}=2.569 a.u., s_B=2.103 a.u.).

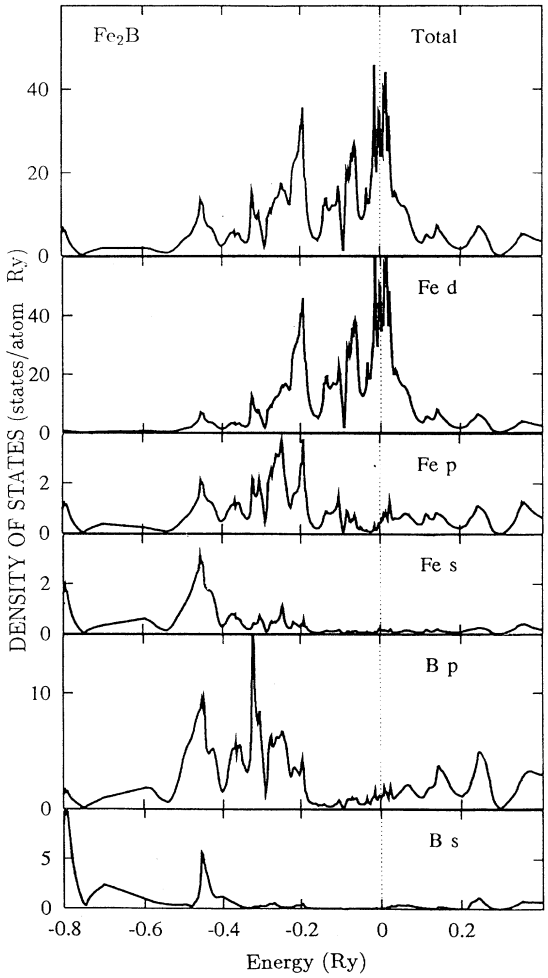

FIG. 2. Paramagnetic density of states of Fe_2B (s_{Fe}= 2.626 a.u., s_B=2.034 a.u.).

racy of the calculated magnetic moments. A mesh of 200–300 nonequivalent k points was used in the irreducible wedge of the Brillouin zone for accurate sampling of the density of states and optical matrix elements. In previous calculations[29] only ten special points were used for the Brillouin-zone sampling at the stage of self-consistent construction of the electron potential; that does not seem accurate enough for calculations of complex metallic crystals with d elements.[28] This might be the reason why the iron moments calculated in Ref. 29 are different from the present values (Table I).

The densities of states in these compounds (Figs. 1–6) do indeed show some universal behavior. The most important aspect is that B keeps only about one s electron in all systems studied, whereas the number of B p electrons is as large as approximately 2 (Table II). It would be expected in a naive ionic picture that B is left with its two s electrons after donating its p electron to a transition metal. On the contrary, we see from Figs. 1–6 that the picture is a strongly covalent one, where the B s states are splitted up into an occupied bonding part with the center of gravity at approximately -0.7 to -0.8 Ry and an empty antibonding part due to interaction with the M s and d orbitals. M d and B p orbitals form a strong bond which results in a large occupancy of B p states and gives a peaked structure in the interval -0.3 to -0.5 Ry. The same picture has been suggested recently Nowak *et al.*[27] for Fe_2B and $Fe_{80}B_{20}$ on the basis of their calculations.

We see in Figs. 1–6 the presence of two main peaks near the Fermi level, separated by about 0.2 Ry, with mainly M d character. The states at the Fermi level in all studied borides have a predominantly nonbonding d character, dividing the whole spectrum into two parts with lower bonding and upper antibonding states.[28] It is known that for most simple crystal structures not all of the d states will have the correct symmetry to form hybrids. This leads to nonbonding states in the compound whose energies are close to the energy of the d band in the element.[36] It is worth mentioning that the partial DOS (PDOS) for the two nonequivalent Fe sites [Fe(1) and Fe(2)] in Fe_3B look very similar (Fig. 3), the

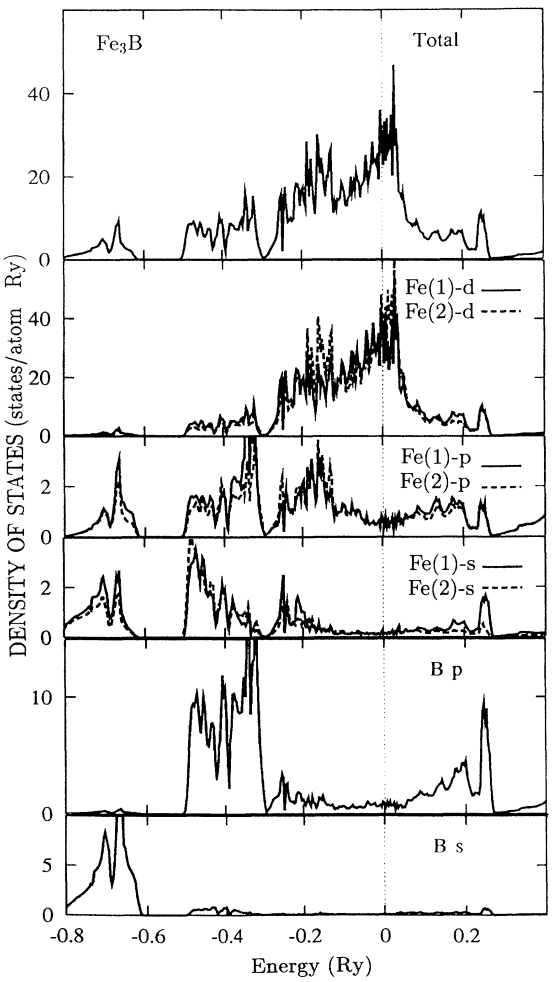

FIG. 3. Paramagnetic density of states of Fe_3B (s_{Fe}= 2.624 a.u., s_B=2.148 a.u.).

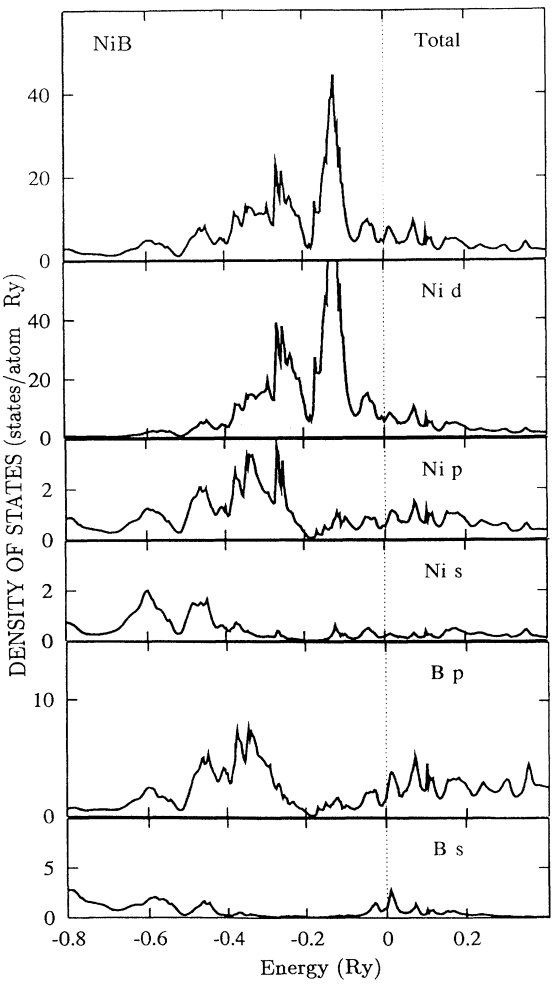

FIG. 4. Paramagnetic density of states of NiB (s_{Ni}=2.555 a.u., s_B=2.092 a.u.).

TABLE I. Magnetic moments (μ_B/atom) on the transition-metal site calculated within the generalized Stoner model in comparison with the ASA-LSDA calculations and experiment.

Compound/site	ASA-LSDA	Gen. Stoner model	Experiment
α-Fe	2.23[a]	2.12	2.217[b]
Fe_3B Fe(1)	1.71[a] 1.91[c]	1.68	
Fe(2)	2.25[a] 2.02[c]	2.14	
average	2.07[a]	1.99	2.0[d] 2.0[e]
Fe_2B	2.13[a] 1.84[f] 1.95[c]	1.89	1.9[d] 1.92[g] 1.91[h]
FeB	1.44[a] 1.25[f] 1.26[c]	1.17	1.12[g] 1.03[h]
Ni_nB	$\leq$0.03[a]	no solution	0[i]

[a]Present work.
[b]Reference 45.
[c]Reference 29.
[d]Reference 9.
[e]Reference 46.
[f]Reference 28.
[g]Reference 8.
[h]Reference 35.
[i]References 10 and 11.

only difference being the presence of some peak on the Fe(2) d PDOS at 0.18 Ry below the Fermi level in comparison with the Fe(1) d PDOS. This might be a result of different Fe-Fe coordination: Fe(1) has two Fe(1) and ten Fe(2) neighbors, whereas Fe(2) has five Fe(1) and six Fe(2) neighbors.[2]

Analysis of the potential in the M sphere shows that it is not very much different from the one in the elemental metals apart from the Madelung shift small compared with the bandwidth, as has been noted for $Fe_{80}B_{20}$ by

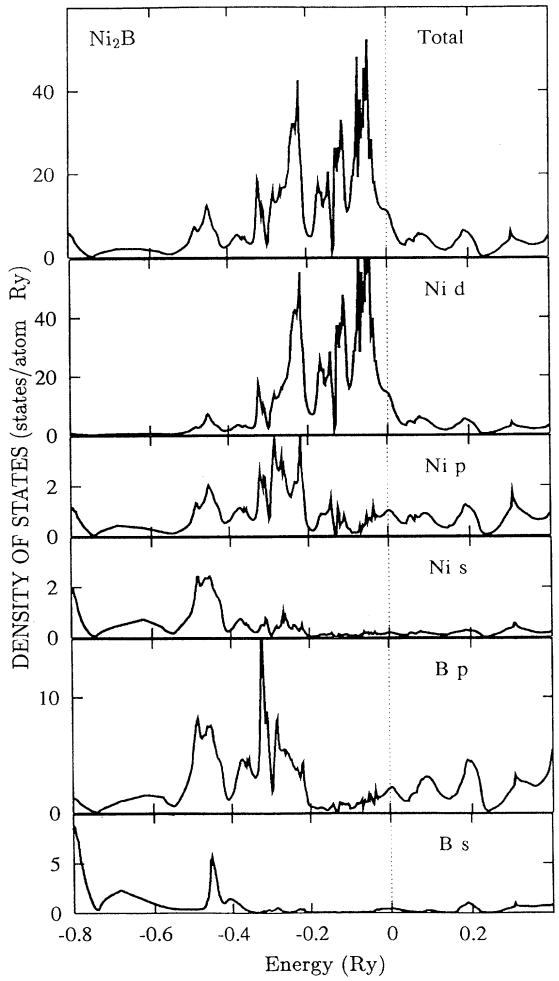

FIG. 5. Paramagnetic density of states of Ni_2B (s_{Ni}= 2.584 a.u., s_B=2.001 a.u.).

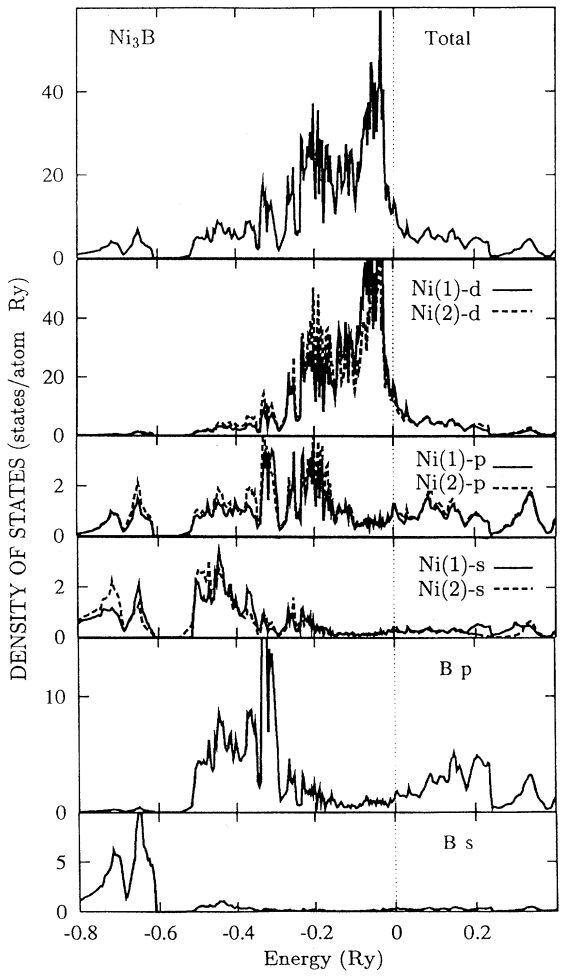

FIG. 6. Paramagnetic density of states of Ni_3B (s_{Ni}= 2.580 a.u., s_B=2.112 a.u.).

TABLE II. Occupation numbers at the Fermi level for Fe-B and Ni-B alloys from the *paramagnetic* calculations (M=Fe,Ni).

Compound/site	$M\,s$	$M\,p$	$M\,d$	Bs	Bp
Fe_3B Fe(1)	0.61	0.89	6.62	0.95	2.09
Fe(2)	0.56	0.78	6.58		
Fe_2B	0.48	0.68	6.51	1.06	2.12
FeB	0.50	0.85	6.73	0.93	2.00
Ni_3B Ni(1)	0.57	0.73	8.63	0.93	1.88
Ni(2)	0.60	0.83	8.70		
Ni_2B	0.48	0.69	8.55	1.07	2.06
NiB	0.58	0.91	8.81	0.95	1.75

Nowak *et al.*[27]. This supports the conclusion that the bonding in the systems studied is predominantly covalent between M and B and metallic between M's.

As a result of the present calculations, we find that in the Ni-B alloys the DOS has practically the same shape as in the iron-boron counterparts (Figs. 4–6). The high-energy Ni d peak is simply shifted downwards with respect to the Fermi level by the addition of two extra d electrons. This is a rather nontrivial result provided we have slightly different actual atomic structures in these two cases. This behavior of the DOS is responsible for the "marginal" behavior of the magnetic moment on Ni as one shifts the Fermi level into a region with low density of states. This behavior can be easily traced with the use of Table II where the occupation numbers are collected. Inspecting the Fe-B series we see that the charge transfers of electrons from B to Fe are small, which shows that they are not very significant characteristics of the bonding. It makes sense, nevertheless, to consider a charge transfer in systems where the M sphere in a compound has nearly the same size as in elemental M, as has been done by Nowak *et al.*[27] for Fe_2B and $Fe_{80}B_{20}$. For Fe_2B simple ASA calculations which give us the charges $z_{Fe} = -0.19$ and $z_B = +0.38$, when no empty spheres is used to mimic the non-muffin-tin effects (to be compared with -0.21 and $+0.42$ obtained in Ref. 27). On the contrary, it was postulated in Ref. 29 that 0.5–0.6 electrons are transferred *from* Fe *to* B, but as we have mentioned before, this is likely to be a result of a just too few k-point sampling of the Brillouin zone (ten special point were used in Ref. 29). Inclusion of empty spheres results in a redistribution of the electron density in close correspondence with the earlier picture of the bonding in iron-boron systems which postulated a valence charge distribution over the whole unit cell.[35] We have also performed full-potential LMTO calculations (see Ref. 38) to keep the contribution to the potential from the nonspherical part of the electron density. As far as the electron density itself is concerned, its nonspherical part can be calculated with high accuracy even when the LMTO calculation employs the atomic-sphere approximation for the one-electron potential.[39] We can see from Fig. 7 that the densities of states calculated for Fe_2B and Ni_2B within the full-potential and ASA methods are indeed very close to each other, differing in some minor details.

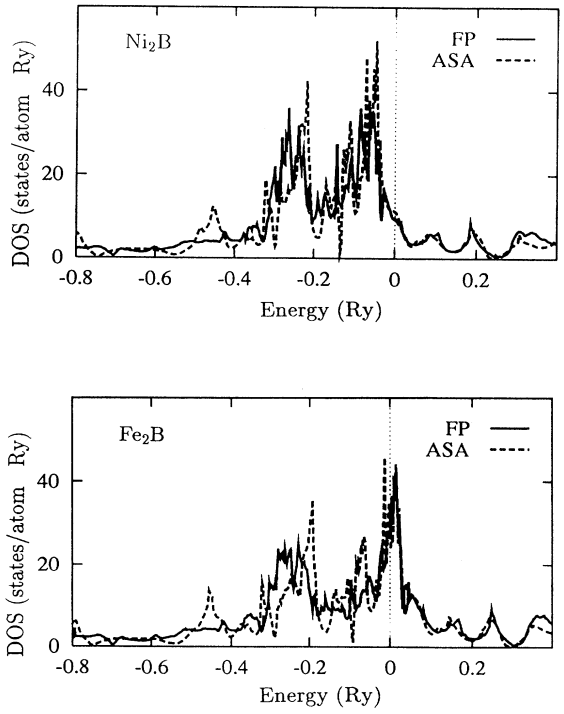

FIG. 7. Paramagnetic DOS for Ni_2B and Fe_2B calculated with ASA-LMTO (solid line) and full-potential LMTO (dashed line).

B. Generalized Stoner model

All studied Fe-B alloys are ferromagnetic and Ni-B alloys paramagnetic as we have mentioned above. To get a simple picture of the ferromagnetic behavior it is convenient to start with the well-known Stoner criterion

$$IN(E_F) \geq 1, \tag{1}$$

where the Stoner parameter I is an atomic parameter, and $N(E_F)$ is the paramagnetic density of states per spin at the Fermi level. This criterion for ferromagnetism does not account for the (paramagnetic) DOS shape near the Fermi level and does not allow one to estimate the actual moment. To make such an estimation we can use the generalized self-consistent Stoner criterion, which for elemental ferromagnets reads[40]

$$I\bar{N}(m) = 1. \tag{2}$$

Here $\bar{N}(m)$ is the DOS averaged over such an energy interval around the Fermi level that gives a moment m. Equation (2) comes simply from a first-order estimate of the perturbation affecting electrons due to the (local) spin polarization $m(\mathbf{r}) = n^{\uparrow}(\mathbf{r}) - n_{\downarrow}(\mathbf{r})$:[40]

$$\Delta V_{\downarrow}^{\uparrow}(\mathbf{r}) = \pm\tfrac{1}{3}\delta(n(\mathbf{r}))\mu_{\mathrm{xc}}(n(\mathbf{r}))m(\mathbf{r})/n(\mathbf{r}), \tag{3}$$

where μ_{xc} is the exchange-correlation potential, and $n(\mathbf{r})$ is the electron density. The exchange splitting $\varepsilon^{\downarrow} - \varepsilon^{\uparrow}$ can be easily expressed via the site- and orbital-projected quantities.[27]

In an actual procedure one defines the Fermi levels $\varepsilon_F^{\uparrow}(m)$ and $\varepsilon_F^{\downarrow}(m)$ in order to satisfy the conditions

$$\frac{1}{2}m = \int_{\varepsilon_F^{\downarrow}}^{\varepsilon_F} N(\varepsilon)d\varepsilon = \int_{\varepsilon_F}^{\varepsilon_F^{\uparrow}} N(\varepsilon)d\varepsilon. \tag{4}$$

Then

$$\bar{N}(m) = m/(\varepsilon_F^{\uparrow} - \varepsilon_F^{\downarrow}) \tag{5}$$

and Eqs. (2), (4), and (5) represent a self-consistent set of conditions giving the value of magnetization. The most important feature of the generalized Stoner model is that it is capable of revealing the actual ferromagnetic behavior even in cases where the standard Stoner condition Eq. (1) fails, as is the case in amorphous $Fe_{80}B_{20}$.[27]

We have analyzed the possible ferromagnetic behavior of $Fe(Ni)_nB$ (n=1,2,3) compounds making use of this generalized Stoner model, only taking into account Fe(Ni) states simply because other contributions around the Fermi level are negligible. Accordingly, all the quantities involved in Eqs. (2), (4), and (5) should be seen as site- and orbital-dependent quantities for the given kind of atom. Simple analysis shows that the solution of Eq. (2) exists only in the case that $N(\varepsilon)$ changes sharply around the Fermi level and has a substantial magnitude. It cannot be satisfied with a flat DOS near E_F.

We have applied the generalized Stoner model to the iron-boron and nickel-boron systems with I=65 mRy for Fe and I=72 mRy for Ni.[40] In the Ni compounds E_F is pushed away from the DOS peaks, which can only result in paramagnetic behavior. The precision of the model in predicting the magnetization in the iron compounds turns out to be rather accurate in comparison with our direct spin-polarized calculations, as follows from Table I.

Even in the case of Fe_3B, where two types of Fe sites exist, the error does not exceed 5% for each site. This means that the generalized Stoner model can be used for a reliable quantitative analysis of possible magnetic behavior.

Comparing the pictures of the spin-polarized DOS (Figs. 8) with the paramagnetic DOS (Figs. 1–3) we can conclude that in all compounds the bands split almost rigidly, with minor changes in the minority spin bands owing to the mechanism of covalent magnetism:[41,28] Namely, the B p band does not follow the splitting of the Fe d band, which increases the energy difference between these states and those of the minority d states, and the Fermi level is pinned above the pure d states. Actually, this competition of different bondings, metallic versus covalent, is hardly seen in Fe_3B and is minor in Fe_2B. Analyzing the trends in magnetic moments in Table I we clearly see that the (average) moment on Fe gradually increases with decreasing boron content, with a clear indication of some sort of saturation at the iron-rich side of the series.

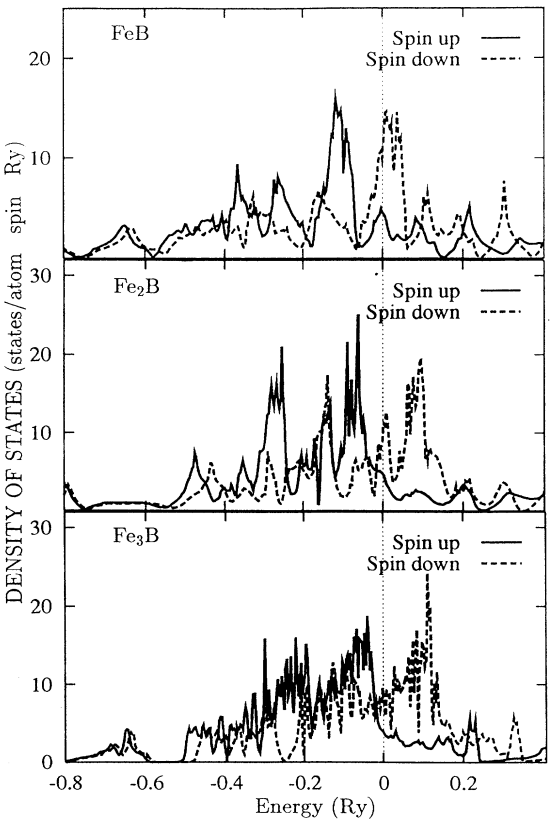

FIG. 8. Spin-projected DOS for FeB, Fe_2B, and Fe_3B.

III. ELECTRON-ENERGY-LOSS SPECTRA

High-resolution uv photoemission, Auger, and EELS measurements for $Fe_{100-x}B_x$ ($0.13 \leq x \leq 0.25$) show that the spectra are not very sensitive to differences in atomic structure between crystals and their amorphous counterparts as well as to the ferromagnetic splitting.[15] To gain more insight into the reasons for this uncommon behavior we have performed first-principles calculations of the EELS for both the para- and ferromagnetic phases of the Fe_nB (n=1,2,3) crystalline alloys making use of the method described earlier.[42,43] For the calculations of the frequency-dependent imaginary part of the dielectric function, $\varepsilon_2(\omega)$, the *spdf* basis for the Fe atom and *spd* basis for the B atom were used. This is essential because the d-f-transitions on the d-element sites are dominant in forming the high-energy plasmon spectra (see discus-

sion in Ref. 42). The real part of the dielectric function $\varepsilon_1(\omega)$ has been computed with the use of the Kramers-Kronig relations. This procedure is accurate only when the imaginary part of the dielectric function is calculated over a wide energy region, and therefore we have calculated $\varepsilon_2(\omega)$ up to energies $\omega \sim 4$ Ry. Intraband (Drude) contributions were also taken into account. In the orthorhombic crystal structure (Fe_3B and FeB compounds) the dielectric function $\varepsilon^{\alpha\beta}(\omega)$ is a tensor, and therefore one must distinguish between three main components of this tensor which correspond to the polarization of the electric field along the a, b, or c axes. In Fe_2B with its tetragonal lattice there could be also a large difference between the ab and the c components of the spectral characteristics.

Figure 9 shows the interband contributions to the optical conductivity $[\sigma^{\alpha\alpha}(\omega) = \varepsilon_2^{\alpha\alpha}(\omega)\omega/4\pi,\ \alpha = a, b, c]$, as well as the real part of the main components of the dielectric tensor for the FeB compound in the paramagnetic phase. As one could have expected, the behavior of the dielectric function is very different for different polarizations in the low-energy region ($\hbar\omega \sim 0$–20 eV). This is not very surprising because the conductivity at $\hbar\omega \sim 1$–7 eV is mainly defined by the transitions between occupied and empty d subbands of Fe. The matrix elements of the momentum operator are nonzero only because of the mixing of states with l=1 and l=3 with the pure d orbitals.[42] In the framework of a tight-binding approximation this mixing appears through overlapping of orbitals localized at the neighboring atoms. The large phase volume for this kind of transition offsets the small value of the matrix elements, and these transitions, therefore, play a crucial role in the low-energy region. It is clear that the shape of the conductivity $\sigma^{\alpha\alpha}(\omega)$ at these energies is very sensitive to the local coordination of a given atom that gives rise to an anisotropy of the dielectric tensor.

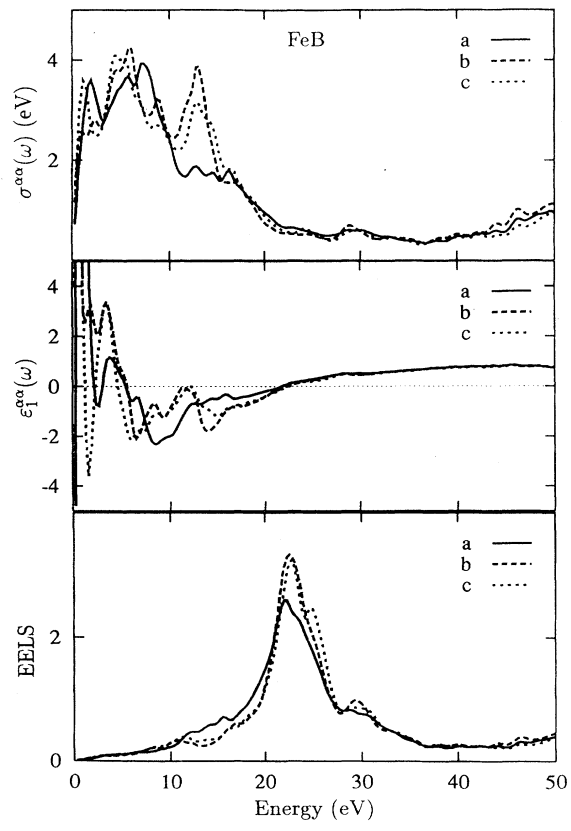

FIG. 9. Optical conductivity $\sigma^{\alpha\alpha}(\omega)$ (upper part), the real part of the dielectric function $\varepsilon_1^{\alpha\alpha}(\omega)$ (middle part), and EELS in FeB for three different polarizations of the electric field.

The intraband transitions play a key role only in the very low-energy region ($\hbar\omega \leq 1$–1.5 eV) because the intraband plasma frequency $\tilde{\omega}_p$, defined by the square of the electron velocity averaged over the Fermi surface, is rather small (of order of 2–3 eV) in all the considered compounds. This is connected with the fact that the Fermi level lies within Fe d bands which are rather narrow. This is characteristic of the M-metalloid compounds including nitrides and carbides.[44]

At energies around 5 eV the interband transitions localized on the B sites begin to play an important role as well as the d-p transitions on the Fe atoms, the latter being also rather anisotropic. In the Fe_nB (n=1,2,3) crystalline alloys the energy region of the d-d transitions localized on the Fe atoms is not well separated from the regions of these new groups of interband transitions, as also happens in the M nitrides and carbides[44] and is a result of strong covalent bonding which mixes all the orbitals in these compounds. As a consequence, the EELS curve in Fig. 9 does not contain any well defined plasmon somewhere between d-d and d-p transition energies as in elemental transition metals.[42] Nevertheless, some indication of the presence of a plasmonlike structure does exist in the region from 10 to 15 eV. These peaks in the EELS are very broad because at the energies where $\varepsilon_1(\omega)$ is close to zero, $\varepsilon_2(\omega)$ is rather large, which results in substantial broadening of this plasmon structure determined by the maximum of the function $L(\omega) = \varepsilon_2(\omega)/[\varepsilon_2^2(\omega) + \varepsilon_1^2(\omega)]$.

At energies higher than 20 eV the difference between different components of $\varepsilon^{\alpha\alpha}(\omega)$ becomes very small. The decrease of the anisotropy of spectra is connected with the fact that the final states for these transitions represent a complicated set of unoccupied B d and Fe f bands. If we have transitions between large clusters of initial and final bands, as happens in the studied borides, there always exist some pairs of bands with a definite symmetry which give rise to a nonzero matrix element of the momentum operator. The behavior of the dielectric function at high energies is rather smooth and the absolute value of the imaginary part $\varepsilon_2(\omega)$ is small in comparison with the low-energy region of intense d-d and d-p transitions. Nevertheless, it is necessary to take this energy region into account also while checking the f-sum rule for $\varepsilon(\omega)$.

The interesting feature of the EELS in Fe_nB (n=1,2,3) is a very strong and well-defined plasmon resonance between 20 eV and 25 eV which differs not too much in energy for all the compounds considered and which does not change its position even in the ferromagnetic state (Fig. 10). It appears close to the energy where $\varepsilon_1(\omega)$ smoothly changes from negative to positive val-

ues and is in the general case rather close to the classical plasma frequency for a homogeneous electron gas $\omega_p^2 = 4\pi N_v e^2/m\Omega$, where N_v is the number of valence electrons and Ω is the volume of the unit cell. Usually, this feature of the EELS is considered as a plasma oscillation involving all of the conduction electrons. Such an interpretation implies that the energy of this peak greatly exceeds the energies for all of the interband transitions. As a matter of fact, the classical plasma frequency in all the considered compounds Fe_nB (n=1,2,3) is practically the same, namely, 29.6 eV for FeB, 30.8 eV for Fe_2B, and 30.7 eV for Fe_3B. We are not in a position to conclude at present whether this coincidence is by chance or not.

Another interesting fact is that the position of the EELS peak is rather far below $\hbar\omega_p$, in contrast to the usual transition metals[42] where this peak is close to the classical plasma frequency. The "softening" of the plasma frequency is connected with the fact that the total oscillator strength of interband transitions with energies greater than ω_p is quite large. This effect can be crudely described by a simplified expression for the energy of the main plasmon from Ref. 42:

$$E_p = \hbar\omega_p[N_{\rm eff}(\omega_p)/N_v]^{1/2}, \tag{6}$$

where $N_{\rm eff}(\omega)$ originates from the f-sum rule,

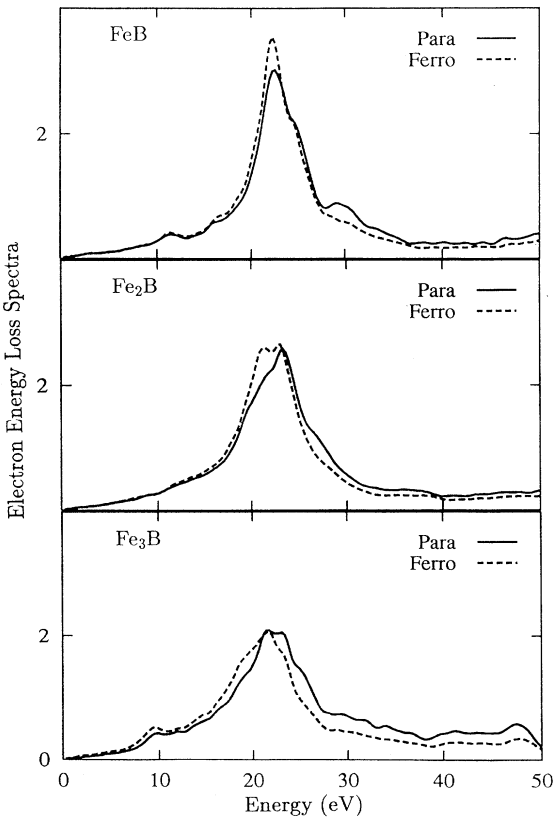

FIG. 10. Energy-loss spectra in paramagnetic and ferromagnetic phases of the crystalline alloys FeB, Fe_2B, and Fe_3B averaged over polarizations.

$$N_{\rm eff}(\omega) = \frac{m\Omega}{2\pi^2 e^2}\int_0^{\omega} d\omega'\omega'\varepsilon_2(\omega'), \tag{7}$$

and gives the oscillator strength for the transitions in a specified energy interval. The approximate formula (6) can be easily derived from the f-sum rule and the Kramers-Kronig relation for the dielectric function $\varepsilon(\omega)$. These characteristics also demonstrate some sort of universal behavior in the considered Fe_nB (n=1,2,3) crystalline alloys. Namely, for all of them the ratio $N_{\rm eff}(\omega_p)/N_v$ is very close to $\frac{1}{2}$, which reflects the crucial role of the high-energy transitions into the empty B d and Fe f bands for both the fulfillment of the f-sum rule and the change of position of the main plasmon maximum. From these simplified formulas we obtain $\hbar\omega_p$=20.85 eV for FeB, 20.57 eV for Fe_2B, and 20.37 eV for Fe_3B in comparison with 22.5, 23.5, and 21 eV from the first-principles LMTO calculations, respectively. Therefore, we conclude that the simple Eq. (6) gives a reasonable quantitative estimate of the position of the main plasmon peak in a paramagnetic phase.

Now we are in a position to explain the behavior of the EELS in the ferromagnetic phase too. The exchange splitting changes the electronic structure mainly around the Fermi level; i.e., it affects only the d band of the transition metal. Therefore this splitting cannot significantly change the EELS even in the energy region below 20 eV because of the same arguments which apply to the paramagnetic case: The main plasmon peak position is fixed by the f-sum rule. At the energies around the main plasmon peak all the interband transitions with large oscillator strengths (which are somewhat different in paramagnetic and ferromagnetic cases) are already saturated and there exists only a smooth background originating from the transitions into the empty B d and Fe f bands. These arguments should provide the reasons for much of the universal behavior of the EELS both in magnetic and nonmagnetic states (Fig. 10) of the M-B compounds.

IV. CONCLUSION

We have presented the results of *ab initio* calculations of the electronic structure and optical properties of two series of crystalline borides: Fe_nB and Ni_nB, n=1,2,3. These results provide a picture of universal trends in bonding in these crystals where the transition metal and metalloid are subject to a strong covalent interaction which decreases with a boron content. Given the metallic bonding between transition-metal atoms, the covalency results in competing interactions affecting the DOS shape. In iron borides the DOS near the Fermi level is dominated by a nonbonding d band which divides the spectrum into bonding low-lying occupied states and high-lying unoccupied antibonding states. The shape of the DOS in nickel borides is very similar to the iron borides apart from a rigid shift of the Fermi level upwards due to the extra two Ni d electrons. The present results show that the picture of charge transfer between the transition-metal atom and metalloid is oversimplified: There is a redistribution of the electron charge over the entire unit cell, with the tendency of an iron atom to

acquire some additional negative charge.

The iron borides are itinerant ferromagnets where the moment on Fe gradually decreases with increasing boron content. This behavior can be qualitatively described by the generalized Stoner model[27] which allows rather accurate determination of the moments. The model involves only the Stoner parameter I, which has an almost atomic character, and the DOS shape near the Fermi level. The model provides insight into the 'marginal' stability of magnetic moment on Ni upon dilution by metalloids.[10,11] On the other hand, the moment on Fe shows some saturation at low dilution, i.e., in iron-rich systems. We expect, therefore, that this behavior should basically survive the effects of disordering, and this indeed follows from the calculations of amorphous systems $Fe_{100-x}B_x$ ($0< x <60$) within the spin-polarized real-space tight-binding LMTO method, where the net iron moment gradually decreases from its maximum net value in hypothetical pure amorphous Fe, which is close to that in elemental bcc iron.[22,23] Thus far we see no evidence for the decreasing Fe moment in iron-rich Fe-B amorphous systems, which has been previously obtained on the basis of semi-empirical Hubbard-model calculations.[17–19] It is worth mentioning that iron-based alloys often show a magnetovolume effect.[4,6] This is believed to be related to ferromagnetic instability and the Invar effect,[47,48] and it would be interesting to investigate this further for M-B alloys.

The admixture of covalent bonding is likely to be responsible for the complicated unit cell of borides and will have some general implications for the optical properties. All of them have a plasmon peak at about 20 eV; this peak is insensitive to ferromagnetic splitting, the effects of crystalline anisotropy are small, and the d-f transitions dominate in the region of the main plasmon peak. These features can be described in terms of the generalized f-sum rule, which immediately demonstrates the importance of the high-energy optical transitions in compounds studied, which are ineffective in elemental transition metals.

The trends we have described in the electronic structure and optical properties of some borides should also hold in a wider class of systems with similar p-d bonding.

ACKNOWLEDGMENTS

We are grateful to Michael Methfessel who provided us with his full-potential code used to calculate the data for Fig. 7. A.M.B. acknowledges fruitful discussions with Volker Heine and David Pettifor.

*Permanent address: P.N. Lebedev Physical Institute, 117924 Moscow, Russia.

[1] R. Kiessling, Acta Chem. Scand. **4**, 146,209 (1950).
[2] W.G. Wyckoff, *Crystal Structures*, 2nd ed. (Wiley, New York, 1965),Vol. 1.
[3] P.H. Gaskell, in *Glassy Metals II*, edited by H. Beck and H.J. Guntherodt (Springer, Berlin, 1983).
[4] E.P. Wohlfarth, J. Magn. Magn. Mater. **7**, 113 (1978); **10**, 120 (1979).
[5] K. Fukamichi, H. Hiroyoshi, M. Kikuchi, and T. Masumoto, J. Magn. Magn. Mater. **10**, 294 (1979).
[6] Z. Xianyu, Y. Ishikawa, S. Ishio, and M. Takahashi, J. Phys. F **15**, 1787 (1985).
[7] J.F. Herbst, Rev. Mod. Phys. **63**, 819 (1991).
[8] M.-C. Cadeville and A.J.P. Meyer, C. R. Acad. Sci. Paris. **255**, 3391 (1962).
[9] M. Takahashi and M. Koshimura, Jpn. J. Appl. Phys. **16**, 1711 (1977).
[10] A. Amamou, F. Gautier, and B. Loegel, J. Phys. F **5**, 1342 (1975).
[11] A. Amamou, D. Aliaga Guerra, P. Panissod, G. Krill, and R. Küntzler, J. Phys. (Paris) Colloq. **41**, C8-396 (1980).
[12] I. Bakonyi, P. Pannisod, J. Durand, and R. Hasegawa, J. Non-Cryst. Solids **61+62**, 1189 (1984).
[13] I. Vincze, D.S. Boudreaux, and M. Tegze, Phys. Rev. B **18**, 4896 (1979).
[14] E.P. Wohlfarth, in *Amorphous Metallic Alloys*, edited by F.E. Luborsky (Butterworths, London, 1983), p. 283.
[15] Th. Paul and H. Neddermeyer, J. Phys. F **15**, 79 (1985).
[16] N. Cowlam and G.E. Carr, J. Phys. F **15**, 1109 (1985); **15**, 1117 (1985).
[17] U. Krey, U. Krauss, and S. Krompiewski, J. Magn. Magn. Mater. **114**, 337 (1992); S. Krompiewski, U. Krey, and H. Ostermeier, *ibid.* **69**, 117 (1987).
[18] H. Ostermeier, W. Fembacher, and U. Krey, Z. Phys. Chem. Neue Folge **157**, 489 (1988).
[19] Y. Kakehashi, Phys. Rev. B **43**, 10820 (1991).
[20] Y.-N. Xu, Y. He, and W.Y. Ching, J. Appl. Phys. **69**, 5460 (1991).
[21] I. Turek and J. Hafner, Phys. Rev. B **46**, 247 (1992).
[22] A.M. Bratkovsky and A.V. Smirnov, J. Phys. Condens. Matter **5**, 3203 (1993).
[23] A. M.Bratkovsky and A.V. Smirnov (unpublished).
[24] O.K. Andersen, Phys. Rev. B **12**, 3060 (1975).
[25] O.K. Andersen and O. Jepsen, Phys. Rev. Lett. **53**, 2571 (1984).
[26] R. Haydock, V. Heine, and M.J. Kelly, J. Phys. C **8**, 2591 (1975).
[27] H.J. Nowak, O.K. Andersen, T. Fujiwara, O. Jepsen, and P. Vargas, Phys. Rev. B **44**, 3577 (1991).
[28] P. Mohn and D.G. Pettifor, J. Phys. C **21**, 2829 (1988); P. Mohn, *ibid.* **21**, 2841 (1988).
[29] W.Y. Ching, Y.-N. Xu, B.N. Harmon, J. Ye, and T.C. Leung, Phys. Rev. B **42**, 4460 (1990).
[30] G. Li and D. Wang, J. Phys. Condens. Matter **1**, 1799 (1989).
[31] J.D. Cooper, T.C. Gibb, N.N. Greenwood, and N.V. Parish, Trans. Faraday Soc. **60**, 2097 (1964).
[32] R. Hasegawa, R.C. O'Handley, L.E. Tanner, R. Ray, and S. Kavesh, Appl. Phys. Lett. **29**, 219 (1976).
[33] R. Hasegawa and R. Ray, J. Appl. Phys. **49**, 4174 (1978).
[34] G. Bayreuther, G. Enders, H. Hoffman, U. Korndörfer, W. Österreicher, K. Röll, and M. Takahashi, J. Magn. Magn. Mater. **31-34**, 1535 (1983).
[35] P.J. Brown and J.L. Cox, Philos. Mag. **23**, 705 (1971); R.S. Perkins and P.J. Brown, J. Phys. F **4**, 906 (1974).
[36] C.D. Gelatt, A.R. Williams, and V.L. Moruzzi, Phys. Rev. B **27**, 2005 (1983).
[37] J.H. Weaver, A. Franciosi, and V.L. Moruzzi, Phys. Rev. B **29**, 3293 (1984).

[38]M. Methfessel, Phys. Rev. B **38**, 1537 (1988); M. Methfessel, C.O. Rodriguez, and O.K. Andersen, Phys. Rev. B **40**, 2009 (1989).
[39]O.K. Andersen, Z. Pawlowska, and O. Jepsen, Phys. Rev. B **34**, 5253 (1986).
[40]O.K. Andersen, O. Jepsen, and D. Glötzel, in *Highlights of Condensed Matter Theory*, edited by F. Bassani, F. Fumi, and M.P. Tosi (North-Holland, New York, 1985).
[41]A.R. Williams, R. Zeller, V.L. Moruzzi, C.D. Gelatt, and J. Kubler, J. Appl. Phys. **52**, 2067 (1981).
[42]I.I. Mazin, E.G. Maksimov, S.N. Rashkeev, and Yu.A. Uspenski, Zh. Eksp. Teor. Fiz. **90**, 1092 [Sov. Phys. JETP **63**, 637 (1986)].
[43]E.G. Maksimov, I.I. Mazin, S.N. Rashkeev, and Yu.A. Uspenski, J. Phys. F **18**, 833 (1988).
[44]A.G. Nargizyan and S.N. Rashkeev, Z. Phys. B **82**, 217 (1991).
[45]L.J. Schwartzendruber, J. Magn. Magn. Mater. **100**, 573 (1991).
[46]H. Bernas, I.A. Campbell and R. Fruchart, J. Phys. Chem. Solids **28**, 17 (1967).
[47]V.L. Moruzzi, Solid State Commun. **83**, 739 (1992).
[48]A.R. Williams, V.L. Moruzzi, C.D. Gelatt, and J. Kübler, J. Magn. Magn. Mater. **31-34**, 88 (1983).